**HEFAT2012**
**9th International Conference on Heat Transfer, Fluid Mechanics and Thermodynamics**
**16 – 18 July 2012**
**Malta**

# EFFECTS OF INTERSTITIAL EXCHANGE PARAMETERS ON THE THERMAL FIELD IN A POROUS CHANNEL WITH HEAT GENERATION AND LOCAL THERMAL NON EQUILIBRIUM

A. Abdedou.[a,b] and K. Bouhadef [*b]
[a] Département du Génie Mécanique, Faculté de Génie de Construction, Université Mouloud Mammeri De Tizi Ouzou, Algerie
[b]USTHB – Faculty of Mechanical and Process Engineering (FGMGP)
Laboratory of Multiphase Transport and Porous Media (LTPMP) - Algeria
E-mail: kbouhadef@usthb.dz and khedbouh@gmail.com

## ABSTRACT

The main objective of this work is to examine the effect of both the solid heat generation ratio, the Biot number and the thermal conductivities ratio on the temperature distributions of both fluid and solid phases and also on the local thermal non equilibrium condition as function of the transverse position and for different section of a porous channel by moving from the inlet to the outlet. The dynamic field in the channel is calculated using the Darcy-Brinkman model and the thermal field is described by the two temperature equations model, which takes into account the local thermal non equilibrium between the two phases by including the interstitial heat transfer between the fluid and solid phases.

The results which emerged from this study mainly revealed that the temperature difference profiles of the two phases change along the channel except for high values of Biot number and conductivity ratio, where they remain almost constant far from the inlet. Moreover, the local thermal equilibrium is fully achieved in the entire channel when the Biot number is high and the conductivity ratio is low, while, conversely, the local thermal non equilibrium is strongly pronounced on the whole field for small values of interstitial Biot number and conductivity ratio.

## INTRODUCTION

The heat transfer inside porous media has attracted the attention of scientists and engineers due to its many engineering applications. Such applications can be found in filtration, geothermal systems, solar energy receiver devices, compact heat exchangers (metal foams), etc. Some configurations involve the heat generation, and include, for this purpose, chemical or nuclear reactors, agricultural and industrial waste storage and electronic components cooling.

When treating a heat transfer problem in porous media, there are basically two different methods commonly found in the literature. One is based on the local thermal equilibrium model, or one equation model, and the other on the local thermal non equilibrium model, also known as two-temperatures equations model. The majority of studies adopt the one equation model which considers that the temperature is the same in both fluid and solid phases, in any point of the porous medium. Plenty of work has been carried out considering the thermal equilibrium model, [1,2] presented a study of transient natural convection in a vertical silo, open at both ends, filled with a porous medium, using the one temperature equation model. These analytical and numerical studies helped to highlight exit conditions to master the dynamic and thermal fields. [3] examined numerically the

## NOMENCLATURE

| | | |
|---|---|---|
| $a_{sf}$ | [$m^2/m^3$] | specific surface area |
| $d_p$ | [m] | pore diameter |
| $h_{sf}$ | [$W/m^2K$] | interstitial heat transfer coefficient |
| $k$ | [W/mK] | Thermal conductivity |
| $K$ | [$m^2$] | permeability |
| $L$ | [-] | dimensionless channel length |
| $p$ | [Pa] | Presseure |
| $P$ | [-] | Dimensionless pressure |
| $Q$ | [$W/m^3$] | volumetric heat generation flux |
| $T$ | [K] | intrinsic average fluid or solid temperature |
| $x$ | [m] | Longitudinal axis direction |
| $y$ | [m] | Transverse axis direction |

Special characters

| | | |
|---|---|---|
| $\rho_f$ | [$kg/m^3$] | fluid density |
| $\mu$ | [kg/m.s] | dynamic viscosity |
| $\nu_f$ | [$m^2/s$] | fluid kinematics viscosity |
| $\theta$ | [-] | dimensionless temperature |
| $\varepsilon$ | [-] | porosity |

Subscripts

| | |
|---|---|
| $f$ | Fluid |
| $p$ | particle |
| $ref$ | Reference value |
| w | wall |
| $s$ | solid |
| 0 | inlet |

optimization of heat transfer of forced convection of non-Newtonian fluid in a parallel plates channel containing porous blocks, using the one equation model. This hypothesis is also adopted by [4] which analyzed the thermal field in the case of forced convection in a plane channel filled with a porous medium in the presence of heat generation, for two types of boundary conditions at the walls (adiabatic walls and heat flux imposed). This model greatly simplifies theoretical and numerical research but the assumption of local thermal equilibrium between the fluid and the solid is inadequate for a number of practical problems. As a result, in recent years more attention has been paid to the local thermal non-equilibrium model, both theoretically and numerically.

The validity of the local thermal equilibrium assumption depends on the value of some thermo-physical parameters of the porous medium and flow conditions. Several researchers have studied the case of local thermal non equilibrium using the two-temperature equations model to assess the intensity of the heat transfer, without taking in consideration the conditions of applicability. Other studies were conducted in order to know in what conditions the thermal non equilibrium model can be applied or not. Thus, [5, 6] studied the conditions and areas of validity of the thermal non equilibrium in the case of forced convection in a horizontal cylindrical pipe. [7] analyzed the phenomenon of the temperature gradient bifurcation (which is defined as the change of sign of the temperature gradient near the wall) between the fluid and solid phases for different types of boundary conditions in the case of the forced convection in the absence of thermal equilibrium and in the presence of local heat generation in the fluid and solid phases. It should be noted that there are no more studies which take account the thermal non equilibrium model with the presence of heat generation in the porous media.

The main objective of this work is to examine the effect of heat generation rate in the solid phase and non dimensional parameters such as Biot number and thermal conductivity ratio on the temperature profile evolution of fluid and the solid phases, as function of the transverse position for different section of the channel by moving from the inlet to the outlet. It will also address the local thermal non equilibrium condition behavior based on these parameters.

## MATHEMATICAL FORMULATION

The study is carried out for a two-dimensional, laminar and permanent flow of an incompressible fluid through a channel, between two parallel plates, of length $\ell$ and width H. The fluid at the channel inlet is assumed to be at uniform velocity $U_0$ and at a constant temperature $T_0$. The walls are maintained at a constant temperature $T_p$ higher than the fluid temperature inlet (Figure1).

The channel is filled by a homogeneous isotropic porous medium with constant porosity and the flow is assumed two-dimensional Cartesian coordinates. The fluid is incompressible and the flow regime is laminar and permanent. It is considered that the thermophysical properties of the fluid do not change with temperature and that that the effects of natural convection and viscous dissipation are negligible.

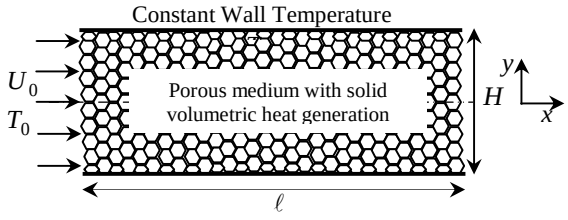


**Figure 1** The physical configuration and Coordinate system

The dynamic field is calculated using the Darcy-Brinkman model and the thermal field is described by the two temperatures equations model, which takes into account the local thermal non equilibrium between the two phases by including the term describing the transfer in both interstitial energy equations. Taking into account the simplifying assumptions above, the steady state governing equations are presented as:

Continuity equation:

$$\vec{v} = 0 \quad (1)$$

Momentum equation :

$$\frac{\rho_f}{\varepsilon}(\vec{v}\nabla)\vec{v} = -\nabla p + \frac{\mu_e}{\varepsilon}\nabla^2\vec{v} - \frac{\mu}{K}\vec{v} \quad (2)$$

Fluid phase energy equation:

$$\varepsilon(\rho c_p)_f\left[u\frac{\partial T_f}{\partial x} + v\frac{\partial T_f}{\partial y}\right] = \varepsilon k_f\left(\frac{\partial^2 T_f}{\partial x^2} + \frac{\partial^2 T_f}{\partial y^2}\right) + h_{sf}a_{sf}(T_s - T_f) \quad (3)$$

Solid phase energy equation:

$$0 = (1-\varepsilon)k_s\left(\frac{\partial^2 T_s}{\partial x^2} + \frac{\partial^2 T_s}{\partial y^2}\right) + (1-\varepsilon)Q - h_{sf}a_{sf}(T_s - T_f) \quad (4)$$

In the present work the expression of $a_{sf}$taken is for a packed bed of spherical particles. It is given by Wakao et al [8] as:

$$a_{sf} = 6\frac{(1-\varepsilon)}{d_p} \quad (5)$$

The study was conducted in order to examine the effect of several dimensionless parameters such as the Biot number and the thermal conductivities ratio, they are highlighted from a set of equations in dimensionless form, which is performed by using the following scaling:

$$X = \frac{x}{H}, \quad Y = \frac{y}{H}, \quad U = \frac{u}{U_0}, \quad V = \frac{v}{U_0}, \quad P = \frac{\varepsilon p}{\rho_f U_0^2}, \quad L = \frac{\ell}{H}, \quad \theta = \frac{T-T_0}{T_p-T_0} \quad (6)$$

The resulting dimensionless continuity, momentum and energy equations are:

$$\frac{\partial U}{\partial X} + \frac{\partial V}{\partial Y} = 0 \quad (7)$$

$$U\frac{\partial U}{\partial X} + V\frac{\partial U}{\partial Y} = -\frac{1}{ReDa}U + \frac{1}{Re}\left(\frac{\partial^2 U}{\partial X^2} + \frac{\partial^2 U}{\partial Y^2}\right) - \frac{\partial P}{\partial X} \quad (8)$$

$$U\frac{\partial V}{\partial X} + V\frac{\partial V}{\partial Y} = -\frac{1}{ReDa}V + \frac{1}{Re}\left(\frac{\partial^2 V}{\partial X^2} + \frac{\partial^2 V}{\partial Y^2}\right) - \frac{\partial P}{\partial Y} \quad (9)$$

$$\frac{\partial \theta_f}{\partial X} + V\frac{\partial \theta_f}{\partial Y} = \frac{1}{PrRe}\left(\frac{\partial^2 \theta_f}{\partial X^2} + \frac{\partial^2 \theta_f}{\partial Y^2}\right) + 6\frac{(1-\varepsilon)}{\varepsilon}\frac{Bi}{PrRe_p}\left(\theta_s - \theta_f\right) \quad (10)$$

$$0 = \frac{\partial^2 \theta_s}{\partial X^2} + \frac{\partial^2 \theta_s}{\partial Y^2} - \frac{6}{\varepsilon}\frac{Bi}{R_k}\frac{Re}{Re_p}\left(\theta_s - \theta_f\right) + \frac{1}{R_k}RQ \quad (11)$$

It can be seen through the above equations the emergence of a several dimensionless groups such as the Reynolds number ($Re = \frac{\rho_f U_0 H}{\mu}$), the Darcy number ($Da = \frac{K}{\varepsilon H^2}$), the thermal conductivities ratio ($R_k = \frac{k_s}{k_f}$), the interstitial Biot number ($Bi = \frac{h_{sf} H}{k_f}$), Prandtl number ($Pr = \frac{\nu_f}{\alpha_f}$) and the dimensionless heat flux ratio($RQ = \frac{Q}{Q_{ref}}$) which is defined as the ratio between the heat generation flux reported in the solid dimensional energy equation (4) and the reference heat flux given by ($Q_{ref} = \frac{(T_w - T_0)k_f}{H^2}$).

In carrying out this investigation, no slip velocity condition is imposed at the solid walls. Also, both fluid and solid phases are assumed in local thermal equilibrium at the inlet and at the channel walls. What is more, the Neumann boundary condition is used here to solve the equations for the upper half of the channel only in order to reduce the computational execution time and storage requirements. Accordingly, the dimensionless boundary conditions can be mathematically expressed as follows:

$$U(0,Y) = 1,\ V(0,Y) = \theta_s(0,Y) = \theta_f(0,Y) = 0 \quad (12)$$

$$U(X,0.5) = V(X,0.5) = 0,\ \theta_s(X,0.5) = \theta_f(X,0.5) = 1 \quad (13)$$

$$\frac{\partial U(X,0)}{\partial Y} = \frac{\partial V(X,0)}{\partial Y} = \frac{\partial \theta_f(X,0)}{\partial Y} = \frac{\partial \theta_s(X,0)}{\partial Y} = 0 \quad (14)$$

$$\frac{\partial U(L,Y)}{\partial X} = \frac{\partial V(L,Y)}{\partial X} = \frac{\partial \theta_f(L,Y)}{\partial X} = \frac{\partial \theta_s(L,Y)}{\partial X} = 0 \quad (15)$$

## NUMERICAL METHOD

The governing dimensionless equations are discretized using the control volume formulation developed by **[9]**. The upwind scheme was used to calculate the convective fluxes across the boundaries of each control volume. Taking into account the structure of the domain, and after tests on the sensitivity to the grid, we chose a grid of 251x121 nodes which is uniform in the both directions (axial and radial). The staggered grid is also used in the current study. Thus, the components, U and V of the velocity are evaluated on meshes shifted downstream in the longitudinal and transverse directions respectively, compared to the principal meshes where the other scalar variables are evaluated. The momentum equations are coupled between them by the intermediary of the pressure field. This difficulty of coupling velocity and pressure comes from the absence of explicit equations which control the pressure field. For this reason, one uses non direct methods as that based on algorithm SIMPLE. The algebraic equations obtained are then solved by using a numerical algorithm based on an iterative SIP (Strongly Implicit Procedure) The relaxation technique is introduced in order to accelerate the convergence of iterations. The dynamic field equations (continuity and movements), which are decoupled from the thermal ones, are solved first until convergence is declared when the relative value of the error between two successive iterations is less than $10^{-6}$. The thermal field (temperature equations of fluid and solid phases) will then be solved until the relative error between two successive iterations is less than $10^{-7}$.

## RESULTS

The study is performed for the case of a porous medium with constant porosity $\varepsilon = 0.9$. The fluid is Newtonian incompressible with a Prandtl number value equal to 0.7. The non dimensional length of the channel for which the calculations were made is L= $\ell$ /H=10. Since the dynamic model chosen is the Darcy-Brinkman model, the value of the Reynolds number based on the particle diameter is assumed equal to unity $Re_p = 1$.

Several criteria have been admitted in the literature to define the local thermal non equilibrium condition. The criterion adopted in this study is that reported by S.A. Khashan et al [5], which is based on the absolute difference in local temperatures of the fluid and solid phases at each point of the computational domain, which is traduced mathematically as:

$$\Delta\theta_{i,j} = \left|\theta_{s_{i,j}} - \theta_{f_{i,j}}\right| \quad (16)$$

It has been well accepted that the condition of local thermal equilibrium holds if $\Delta\theta_{i,j} \leq 0.05$ and inversely, the local thermal non equilibrium is so pronounced if $\Delta\theta_{i,j} > 0.05$. The objective of this criterion is to show the spatial distribution of the local thermal non equilibrium (or equilibrium) over the channel length. So from this test we can delineate the areas of the channel where there is local thermal equilibrium and the areas where there is local thermal non equilibrium. The maximum value of the absolute local temperature difference between the fluid and solid phases in the entire channel can serve as another criterion for examining the effect of such dimensionless parameters on the LTNE condition defined as [6]:

$$LTNE = max(\Delta\theta_{i,j}) \quad (17)$$

The results are presented and discussed in terms of the fluid and solid temperatures difference and LTNE condition profiles. In the first part of the results, the plots show the effect of governing parameters such as the Biot number and the conductivity ratio on the LTNE condition. The second part of the results reported in this work concerns the evolution of the temperature difference profiles between the fluid and solid phases over the channel length from the inlet to the outlet.

**Biot number and thermal conductivity ratio effects on the TLNE condition**

Figs. 2 & 3 display the impact of Biot number on LTNE condition which represents, as mentioned by equation (17), the maximum value of absolute difference between the temperature of solid and fluid phases at all point in the channel. The results are presented for different values of solid-to-fluid thermal conductivity ratio $R_k$. The curves show that the increase in the interstitial Biot number led to a reduction in the magnitude of the maximum LTNE values for the both cases (with and

without heat generation). This due to the increase in the internal heat transfer between the two phases.

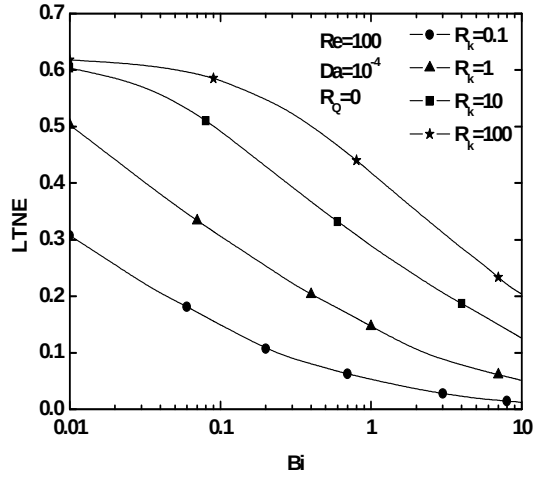


**Figure 2** Impact of solid-to-fluid thermal conductivity ratio on LTNE condition at different Biot number, Re=100, Da=$10^{-4}$ and RQ=0

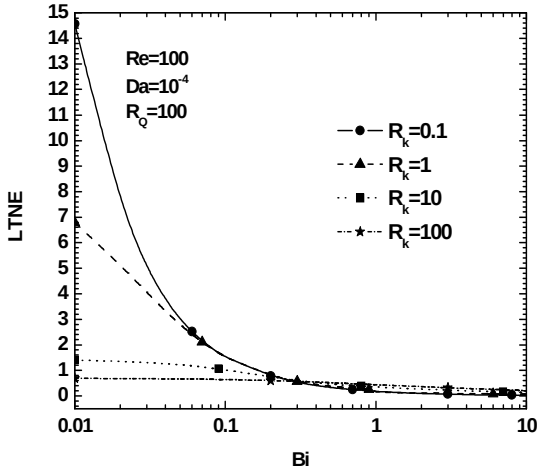


**Figure 3** Impact of solid-to-fluid thermal conductivity ratio on LTNE condition at different Biot number, Re=100, Da=$10^{-4}$ and RQ=100

The effect of the thermal conductivity ratio on the local thermal non equilibrium condition depends on whether there is heat generation or not. In the case of the absence of heat generation (Figure 2), the increase in the conductivity ratio increases the LTNE while keeping the look decreasing with increasing Biot number. As a low value of the conductivity ratio corresponds to a high value of the fluid conductivity, the heat transfer is clearly dominated by conduction in the fluid thereby reducing the LTNE between the two phases. Gradually, as the conductivity ratio increases, the fluid conductivity decreases in favor of that of the solid phase, which causes the heat transfer to be achieved mainly by conduction in the solid and consequently increase the local thermal non equilibrium.

When the heat generation is important, Figure 3 shows that the LTNE decreases with increase in interstitial Biot number for all values of the thermal conductivity ratio. This reduction in the LTNE is due to the increase in internal heat transfer between the two phases, evacuating thereby the heat generated in the solid phase to the fluid phase. For low values of $R_k$ and Bi, the LTNE reached very high values, which is the consequence of the high thermal resistance in the solid phase (low values of $R_k$) and high internal thermal resistance (low Bi), thus preventing the evacuation of the high amount of heat generated in the solid phase over both sides. By increasing the thermal conductivity ratio, it was found that the LTNE tends to decrease up until a certain value of Biot number, from which the trend starts to reverse (increasing LTNE with the increase in $R_k$). The low values of Bi prevent the evacuation of heat generated in the solid phase, hence the significant increase in its temperature and hence the high value of LTNE condition. The increase in the conductivity ratio leads to an increase in the ability of the solid to evacuate some of the generated energy, by conduction through the solid wall with a possible reversal in the heat transfer direction. When Bi increases, the internal heat exchange becomes important and the heat generated is evacuated more from the solid phase to fluid phase which is discharged to the outside. In this case, any increase in $R_k$ causes the increase of thermal resistance in the fluid in favor of that of the solid phase, leading to reduce the transfer by conduction in the fluid and thus to increase the LTNE.

Figures 4 & 5 show the effect of the thermal conductivity ratio on the LTNE for various values of Biot number. In the case of the absence of heat generation, Fig. 4 indicates that the LTNE increases with the increase in the conductivity ratio for all values of the Biot number. The intensity of LTNE diminishes significantly the Biot number augments, due the increase of internal heat transfer between the two phases.

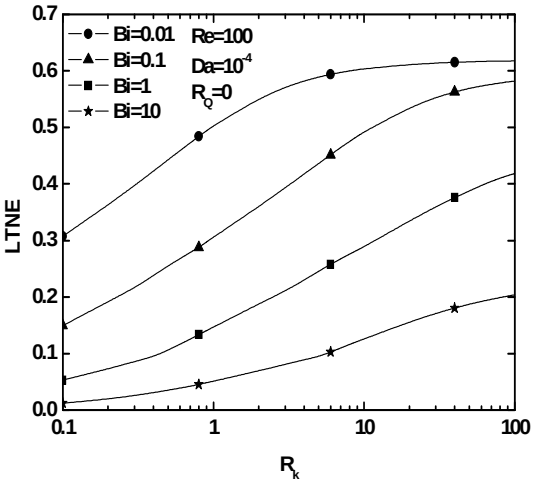


**Figure 4** Impact of interstitial Biot Number on LTNE condition at different conductivity ratio, Re=100, Da=$10^{-4}$ and RQ=0

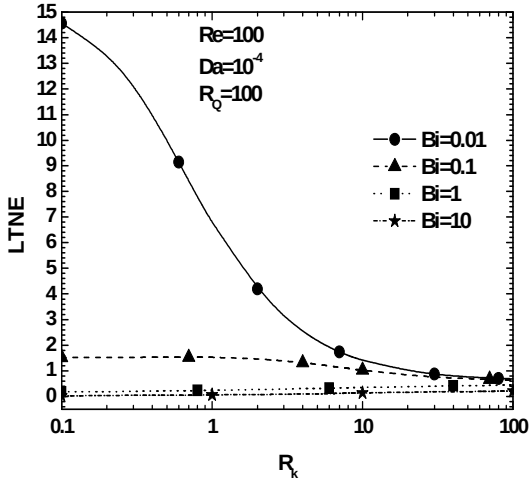


**Figure 5** Impact of interstitial Biot Number on LTNE condition at different conductivity ratio, Re=100, Da=$10^{-4}$ and RQ=100

The presence of heat generation in the solid phase changes the effect of the conductivity ratio on the LTNE, as shown in Figure 5. Thus, for low values of the Biot number (Bi = 0.01, 0.1), the LTNE decreases along the lines of increasing values of the thermal conductivity ratio. When increasing the Biot number (Bi = 1 & 10), one can see that the effect of the conductivity ratio on the LTNE is reversed so that the increase in $R_k$ increases the LTNE. The energy generated in the solid is removed, in large part by internal heat exchange with the fluid phase (high values of Bi), thus any increase in $R_k$ results in an increase in the conductivity of the solid and therefore an augmentation in the conductive heat transfer received by the solid from the wall.

**Biot number and thermal conductivity ratio effects on the temperature difference distribution**

Figs. 6 & 7 displays the absolute temperatures difference distribution between the solid and fluid phases, as mentioned by equation (16), as function of transverse coordinate for different axial positions over the channel length for a low value of Biot number (Bi=0.01) for different values of solid-to-fluid thermal conductivity ratio $R_k$. As shown in Figure 6, the difference between the temperatures of the two phases is highly enhanced from zero value, due to the imposed condition of local thermal equilibrium at the wall, towards the channel centre value. It appears, also, that the temperature difference between the two phases is the largest in the inlet region, decreasing gradually with the evolution downstream. In fact, one can easily notice that, in the considered case (high heat generation in the solid phase) the local thermal non equilibrium is strongly pronounced in any point with maximum values on the central axis of the channel.

For a high value of thermal conductivity ratio (Figure 7), one can notice that the value of the temperature difference between the two phases presents a high increase in the inlet zone particularly in the vicinity of the wall. This difference decreases substantially thereafter due to the solid phase cooling, and when moving towards the exit of the channel. This behavior can be attributed to the increase in the temperature of the fluid which receives the heat from the wall gradually as one move downstream and can be explained by the fact that high value of the thermal conductivity ration allows heat generated in the solid to be conducted over the solid phase to the wall even going in the opposite direction of the initial heat flux.

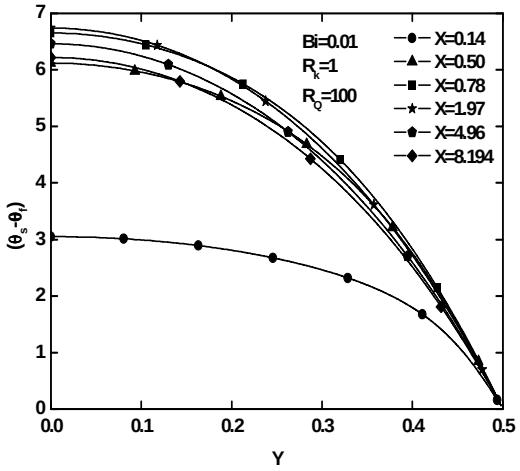


**Figure 6** Temperature difference profile as a function of transverse distance at different axial positions, Re=100, Da=$10^{-4}$ , RQ=100, Bi= 0.01 and $R_k$=1

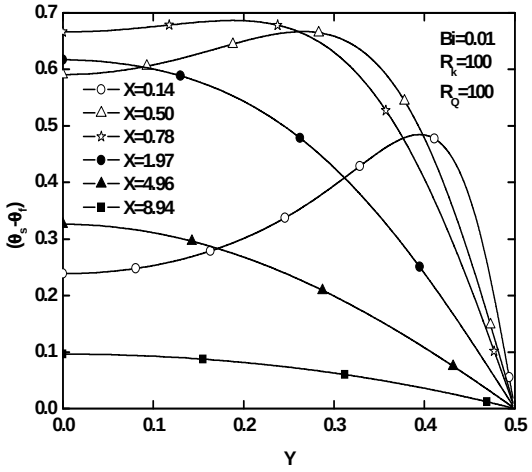


**Figure 7** Temperature difference profile as a function of transverse distance at different axial positions, Re=100, Da=$10^{-4}$ , RQ=100, Bi= 0.01 and $R_k$=100

When Biot number takes a high value (Bi=10), and for a low value of conductivities ratio (Figure 8), the profile of the temperature difference between the two phases reaches very low values, what this is direct result of good internal thermal communication between the two phases (high Bi). This difference is smaller when we move over the channel to the outlet. So by examining the values of this temperature difference between the two phases, we can easily say that the

local thermal equilibrium condition is satisfied, in this case, over the entire channel under study.

At this same high Biot number, when the of thermal conductivities ratio also takes high values (Figure 9), we find that the representation of the temperature difference between the two phases shows a relative high value at the channel inlet and decrease become constant and almost negligible in advancing downstream of the channel. Here again, we see that the condition of local thermal equilibrium is strongly checked on the whole channel except the inlet region. The significant increase in the conductivity of the solid allows a part of the generated heat to be evacuated by conduction in the solid and another part is evacuated by internal transfer to the fluid (high Bi) and then by convection to outside.

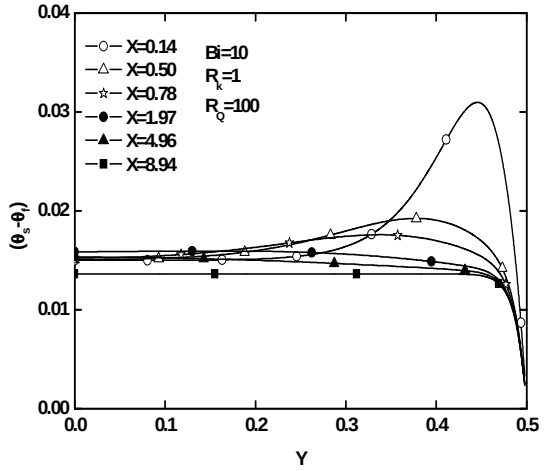


**Figure 8** Temperature difference profile as a function of transverse distance at different axial positions, Re=100, Da=$10^{-4}$ , RQ=100, Bi= 10 and $R_k$=1

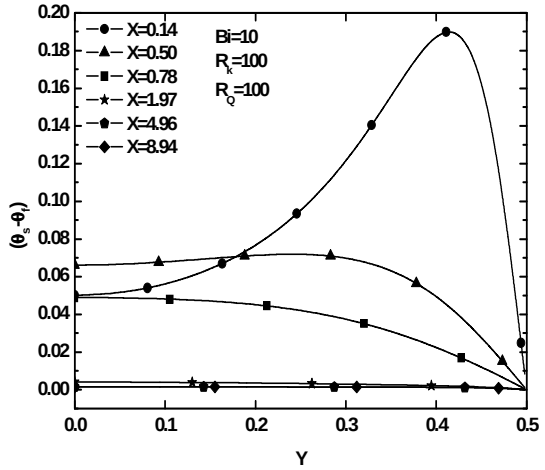


**Figure 9** Temperature difference profile as a function of transverse distance at different axial positions, Re=100, Da=$10^{-4}$ , RQ=100, Bi= 100 and $R_k$=100

## CONCLUSION

The present study is a numerical analysis of forced convection in a plane channel filled with a porous medium in the presence of heat generation in the solid, the main objective being to identify and treat conditions of applicability of local thermal equilibrium condition within the porous medium. The effect of parameters such that the thermal conductivity ratio and the local Biot number, reflecting the interstitial exchange, on the temperature difference profiles of these phases and on the condition of local thermal equilibrium, was examined. The main results emerged from this study revealed that:

• The value of the temperature difference which can significantly increase in the inlet region of the channel will diminish with distance downstream.

• The local thermal equilibrium is perfectly realized over the entire length of the channel when the interstitial exchange (Bi) is high and the thermal conductivity ratio ($R_k$) is low, while, conversely, the local thermal non equilibrium is strongly pronounced in the entire channel for small values of Bi and $R_k$.

• When Bi and $R_k$ are both of high values, the local thermal equilibrium is achieved over a major part of the channel except in the inlet region.

## REFERENCES


[1] D.E. Ameziani, R. Bennacer, K. Bouhadef, A. Azzi, Effect of the days scrolling on the natural convection in a open ended storage silo, *International Journal of Thermal Sciences 48 (2009) 2255-2263.*

[2] D.E. Ameziani, R. Bennacer, K. Bouhadef, O. Rahli, Analysis of the chimney natural convection in a vertical porous cylinder. *Numerical Heat Transfer, Part A applications, Vol 54, pp47-66, 2008.*

[3] R. Nebbali, K. Bouhadef, Non-Newtonien fluid flow in plane channels: Heat transfer enhancement using porous blocks, *International Journal of Thermal Sciences 50 (2011) 1984-1995.*

[4] G.M. Chen, C.P. Tso and Yew Mun Hung, Field synergy principle on fully developed forced convection in porous medium with uniform heat generation, *international communications in Heat and Mass Trasfer 38 (2011) 1247-1252*

[5] S.A. Khashan, A.M. Al-Amiri, M.A. Al-Nimr, Assessment of the local thermal non-equilibrium condition in developing forced convection flows through fluid-saturated porous tubes, *Applied Thermal Engineering 25 (2005) 1429-1445.*

[6] S.A. Khashan, A.M. Al-Amiri, I. Pop, Numerical simulation of natural convection heat transfer in a porous cavity heated from below using a non-Darcian and thermal non-equilibrium model, *Int. J Heat Mass Transfer 49 (2006) 1039-1049*

[7] Kun Yang, Kambiz Vafai, Analysis of temperature gradient bifurcation in porous media- an exact solution, *Int. J Heat Mass Transfer 53 (2010) 4316-4325.*

[8] N. Wakaoo, S. Kaguei and T. Funazkri, Effect of fluid dispersion coefficients on particle to fluid heat transfer coefficients in packed beds, *Chem. Engng Sci. 34, 325-336 (1979).*

[9] Patankar S. V, "Numerical heat transfer and fluid flow", Hemisphere, New York.1980.